Compressive Diffusion MRI – Part 1: Why Low-Rank?

Hao Gao[1,2], Longchuan Li[3], and Xiaoping Hu[3]

[1]*Department of Mathematics and Computer Science, Emory University, Atlanta, Georgia, United States,* [2]*Department of Radiology and Imaging Sciences, Emory University, Atlanta, Georgia, United States,* [3]*Department of Biomedical Engineering, Emory University and Georgia Institute of Technology, Atlanta, Georgia, United States*

Purpose: The applications of compressive sensing [1,2] in MRI have been actively studied since 2006 [3]. The purpose of this work is to compare several sparsity models for dynamic MRI with the focus on the diffusion MRI. An important factor that affects their performance is that the diffusion-weighted (DW) images (x-q) are often correlated along the DW dimension, which can be mathematically characterized as low-rank when each DW image is aligned as a column vector with q as the matrix row index (Fig. 1).

Methods: (1) The first dynamic sparsity model under comparison is the 1D pixel-wise Fourier transform (FT) along the DW dimension from the DW image space (x-q) to the DW frequency space (x-f), which was similar to the sparsity models in k-t SPARSE [4] and k-t FOCUSS [5]. Here a notable difference is that the x-f counterparts of x-q images are not as sparse as those of x-t images. (2) The second is the local sparsity up to some transform (e.g., total variation (TV) or wavelet) [3]. Here we adopt the tensor framelet (TF) [6] that naturally generalizes the TV and the wavelet. (3) The third one is the adaptive sparsity through dictionary learning (DL) [7]. Here we assume the ideal case that the dictionary is constructed from the DW images to be reconstructed. (4) The fourth one is the global sparsity via the low-rank model (LR) that involves SVD as utilized in partially separable functions [8] and k-t PCA [9]. (5) The fifth one is the supposition of the local sparsity and the global low-rank sparsity [10]. Here we jointly apply LR and TF (LR+TF). (6) The last one is the rank-sparsity decomposition (RSD) [11]. Although RSD may also involve LR and TF, its approach is very different from LR+TF.

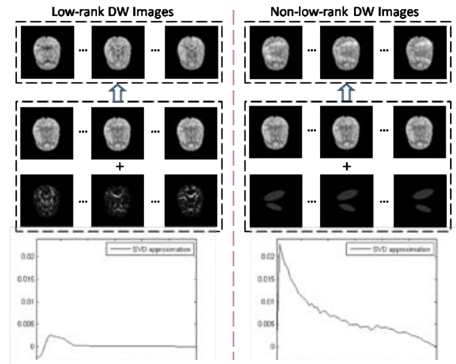

Fig. 1. The DW images are often low-rank, and thus can be approximated well by its principal components through SVD. In contrast, the non-trivial difference between the non-low-rank DW images and their SVD approximation remains.

Results: The DW images were reconstructed (Figs. 2-4) with the above models (1)-(6) solved by the split Bregman algorithm [12] with the same stopping criterion (i.e., the relative difference from iteration to iteration). Here the reconstructions are with 60 DW directions (D=60), SNR=30, various b values (i.e., b=1000, 2000, and 3000), 4-fold and 8-fold k-space undersampling respectively. For (c)-(e) in Fig 2-4, the 1st row consists of the reconstructed images represented in a DW direction (x-y), the central x-slice with all DW directions (x-q), the central y-slice with all DW directions (y-q), and the zoom-in detail of the ROI; the 2nd row consists of their differences from the original images. Figs. 2 and 3 indicate that LR led to the smallest reconstruction error (i.e., $||X\text{-}X_0||/||X_0||$) and the best image quality, and RSD led to the second best. However, when the DW images are non-low-rank (Fig .4), RSD is the best in terms of both the reconstruction error and the image quality.

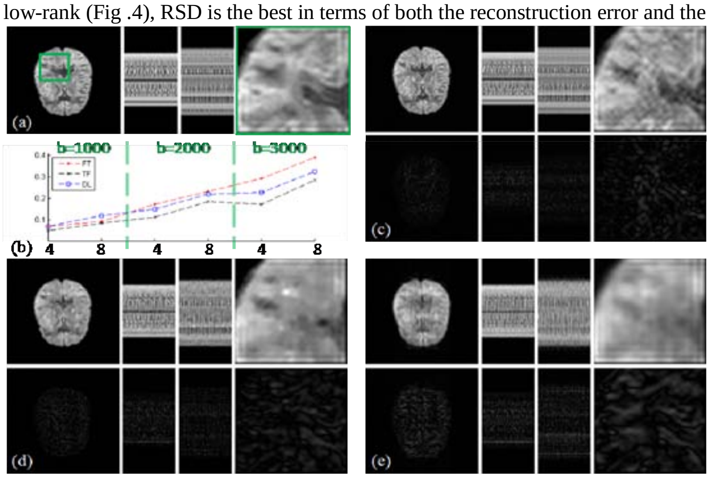

Fig. 2. Image reconstruction via FT, TF, and DL. (a) The gold standard. (b) Reconstruction errors. (c) FT, (d) TF, and (e) DL with 8-fold undersampling.

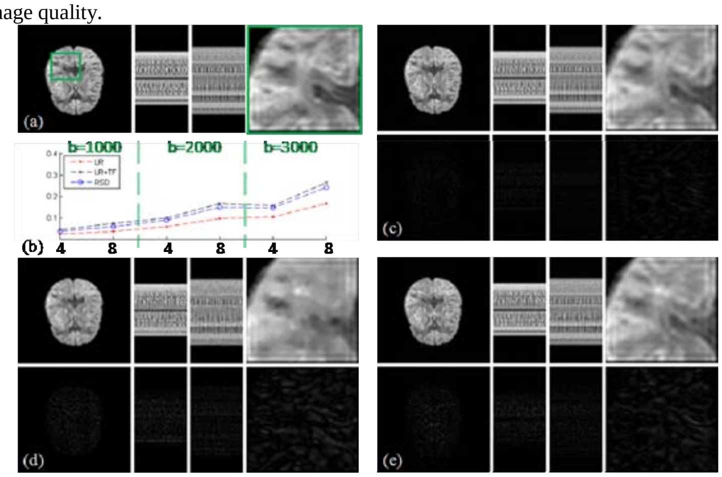

Fig. 3. Image reconstruction via LR, LR+TF, and RSD. (a) The gold standard. (b) Reconstruction errors. (c) LR, (d) LR+TF, and (e) RSD with 8-fold undersampling.

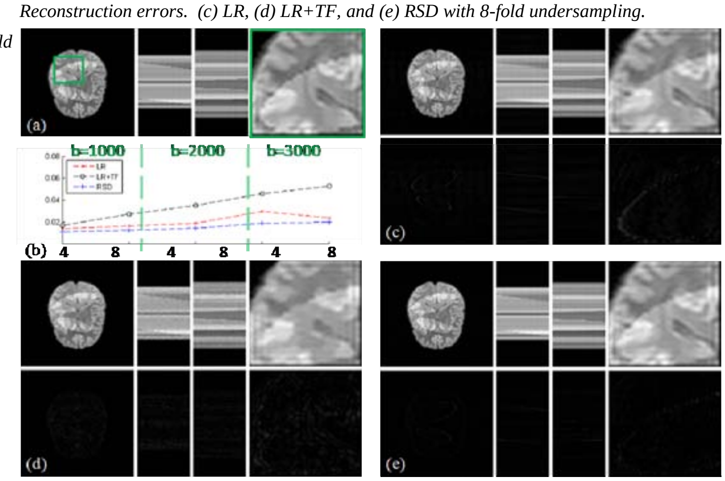

Fig. 4. Image reconstruction via LR, LR+TF, and RSD for non-low-rank DW images. (a) The gold standard. (b) Reconstruction errors. (c) LR, (d) LR+TF, and (e) RSD with 8-fold undersampling.

Conclusion and Discussion: Since the DW images are often low-rank (Fig. 1), the LR model, a global sparsification of DW images via SVD, generally provides the best image reconstruction (Figs. 2-3), while the rank-sparsity decomposition is the best (Fig. 4) when the DW images are non-low-rank. On the other hand, we observed that the performance LR+TF falls between those of LR and TF, likely suggesting that the better of LR and TF should be used instead of LR+TF. Note that the present study did not take into account the phase change due to the varying diffusion gradient, which could be problematic and certainly should be minimized.

References: 1. Candès et al, *IEEE Trans. Inf. Theory*, 52, 489-509 (2006); 2. Donoho, *IEEE Trans. Inf. Theory*, 52, 1289-1306 (2006); 3. Lustig et al, *MRM*, 58, 1182-1195 (2007); 4. Lustig et al *ISMRM*, 2420 (2006); 5. Jung et al, *MRM*, 61, 103-116 (2009); 6. Gao et al, *Med. Phys.*, 39, 6943-6946 (2012); 7. Ravishankar and Bresler, *IEEE Trans. Med. Imaging*, 30, 1028-1041 (2011); 8. Liang, *IEEE ISBI*, 988-991 (2007); 9. Pedersen et al, *MRM*, 62, 706-716 (2009); 10. Goud et al, *IEEE ISBI*, 988–991 (2010); 11. Gao et al, *CAM Report* 11-26 (2011); 12. Goldstein and Osher, *SIAM J. Imaging Sci.*, 2, 323-343 (2009).